Am J Physiol Lung Cell Mol Physiol 287: L1284–L1292, 2004.
First published August 20, 2004; doi:10.1152/ajplung.00177.2004.

Inhibition by cytoplasmic nucleotides of a new cation channel in freshly isolated human and rat type II pneumocytes

Norbert Mair,[1] Manfred Frick,[1] Cristina Bertocchi,[1] Thomas Haller,[1] Albert Amberger,[2] Helmut Weiss,[3] Raimund Margreiter,[2,3] Werner Streif,[4] and Paul Dietl[1]

Departments of [1]Physiology, [3]General and Transplant Surgery, and [4]Pediatrics, Medical University of Innsbruck, and [2]Tyrolean Cancer Research Institute, A-6020 Innsbruck, Austria

Submitted 17 May 2004; accepted in final form 12 August 2004

Mair, Norbert, Manfred Frick, Cristina Bertocchi, Thomas Haller, Albert Amberger, Helmut Weiss, Raimund Margreiter, Werner Streif, and Paul Dietl. Inhibition by cytoplasmic nucleotides of a new cation channel in freshly isolated human and rat type II pneumocytes. *Am J Physiol Lung Cell Mol Physiol* 287: L1284–L1292, 2004. First published August 20, 2004; doi:10.1152/ajplung.00177.2004.—Here we report a 26- to 29-pS cation channel abundantly expressed in freshly isolated and primary cultured type II cells from rat or healthy human lungs. The channel was never spontaneously active in cell-attached patches but could be activated by cell permeabilization with β-escin. Excised patch-clamp experiments revealed activation by Ca^{2+} concentrations at the cytoplasmic side in the micromolar range. High concentrations of amiloride (>10 μM) at the extracellular side did not inhibit. The channel was equally permeable for K^+ and Na^+ but was essentially impermeable for Cl^-, Ca^{2+}, and Mg^{2+}. It was blocked by adenosine nucleotides (cytoplasmic side) with the following order of potency: AMP ≈ ADP ($EC_{50} \leq 10$ μM) > ATP ≫ adenosine ≫ cyclic AMP. The blocking effect of ATP was reproduced by its nonhydrolyzable analogs AMPPNP or ATP-γ-S. GTP did not inhibit. Cd^{2+} blocked the channel with an $EC_{50} \approx 55.5$ nM. We conclude that type II cells express a Ca^{2+}-dependent, nucleotide-inhibited, nonselective, and Ca^{2+}-impermeable cation channel ($NSC_{Ca/AMP}$) with tonically suppressed activity. RT-PCR confirmed expression of TRPM4b, a channel with functional characteristics almost identical with $NSC_{Ca/AMP}$. Potential physiological roles are discussed.

patch clamp; calcium; adenosine 5′-monophosphate; adenosine 5′-diphosphate; adenosine 5′-triphosphate; cadmium; lung; alveolus; nonselective cation channel

ION CHANNELS in alveolar type II cells have been intensively investigated. Most attention has been directed toward ion channels involved in transepithelial solute and water transport, one reason being the fascinating transition of the alveolus from a secretory to a reabsorptive organ during birth (reviewed in Ref. 32). Although the cellular mechanisms and physicochemical processes of this transition are still only partly understood, the general concept emerged that both secretion and reabsorption are active processes of the type II cell, the latter being dependent on the expression of functional α-subunits of the epithelial Na^+ channel (ENaC) (11). Also in the adult alveolus, ion transport through type II cells is considered to play an essential role for alveolar fluid balance and edema clearance (reviewed in Ref. 25), although recent evidence suggests that type I cells may contribute to this task (14).

Substantial controversy has recently evolved about the role of Cl^- channels as well as the molecular identities, biophysical properties, and regulation of Na^+ channels involved in transepithelial NaCl reabsorption in the adult alveolus (reviewed in detail in Refs. 20, 23, 24, 28, and 40). A particular matter of debate is a heterogeneous group of poorly selective cation channels, which have been described by several groups in both fetal distal epithelial (29) and adult type II cells (1, 5, 12, 13, 15, 36, 42). These channels have conductances between 10 and 30 pS and are differently sensitive to elevations of Ca^{2+} concentrations at the cytoplasmic side ($[Ca^{2+}]_{cyt}$). Some of them are considered to be associated with ENaC-mediated, transepithelial solute transport for several reasons. First, they are generally inhibited by high concentrations of amiloride, which also blocks ENaC and perinatal fluid reabsorption. Second, channel activity was reported to be stimulated by cyclic AMP or protein kinase A (1, 3, 36, 42), which is also thought to be the major signaling pathway of epinephrine-stimulated fluid reabsorption and perinatal fluid clearance. Third, and most specifically, antisense oligonucleotides targeting the α-subunit of ENaC decreased the density of the 20.6-pS, nonselective cation channel (12). As for all ENaC-related cation channels, ion selectivity may be determined by the coexpression pattern of the three subunits (7, 35, 37), giving rise to substantial functional diversity, depending on culture conditions and delay after isolation from lung tissue (13, 41). Another class of cation channels, activated by cyclic GMP, was suggested to account for an amiloride-insensitive fraction of alveolar fluid clearance (27).

Here we describe another, yet unknown, cation channel in the alveolar type II cell. This channel is most likely not involved in transepithelial solute transport, as it is amiloride insensitive and not activated by compounds known to stimulate epithelial transport. Consistently, channels with similar features have been described in various nontransporting and transporting cell types (10, 16, 30, 33, 34, 38). Adopting the classification of Halonen and Nedergaard (10), we refer to it as $NSC_{Ca/AMP}$, because Ca^{2+} is the only known activator and AMP (together with ADP) has the most potent blocking effect. Its high abundance in freshly isolated human and rat type II pneumocytes suggests an important function that remains to be determined.

METHODS

Rat type II cell preparation. This was done according to the method of Dobbs et al. (4), with minor modifications (9). At the end of the cell preparation from adult male Sprague-Dawley rats (~200 g), type II

Address for reprint requests and other correspondence: P. Dietl, Dept. of Physiology, Medical Univ. of Innsbruck, Fritz-Pregl-Str. 3, A-6020 Innsbruck, Austria (E-mail: paul.dietl@uibk.ac.at).

The costs of publication of this article were defrayed in part by the payment of page charges. The article must therefore be hereby marked "*advertisement*" in accordance with 18 U.S.C. Section 1734 solely to indicate this fact.

Table 1. *Summary of features of cation channel tested in both rat and human alveolar type II cells*

Alveolar Type II Cell	Excision Activation, Ca^{2+} Dependence	Nonselective for Na^+, K^+	Cytoplasmic ATP Inhibits	Cytoplasmic ADP Inhibits	Cytoplasmic AMP Inhibits	Extracellular ATP, (−)Isoproterenol Activates
Rat	yes	yes	yes	yes	yes	no
Human	yes	yes	yes	yes	yes	no

Excision activation denotes an open probability = 0 in the cell-attached patch-clamp configuration but channel activation after changing from the cell-attached to the inside-out mode in the presence of 2 mM Ca^{2+} in the bath solution.

cells were suspended in DMEM supplemented with 10% FCS, 100 U/ml penicillin, 100 μg/ml streptomycin, and 24 mmol/l $NaHCO_3$ and seeded on glass coverslips at low density (~40 cells/mm^2). Cells were given time to settle in 95% humidified air plus 5% CO_2 (37°C) for 6–48 h before being used for patch clamp.

Human type II cell preparation. Human type II cells were obtained from cadaveric donor lung lobes that were not considered suitable for lung transplantation due to adjacent organ injury. Lung preservation was carried out according to standardized protocols for human organ transplantation. In brief, lower pulmonary lobes were retrieved as part of multiorgan procurement (22). A median sternotomy was performed, and all of the abdominal dissections were finished before lung perfusion was started. After heparin administration, the lower lobe was completely inflated and resected by use of a staple-line instrument (Endo-GIA; Tyco Healthcare, Vienna, Austria). The respective pulmonary artery was then cannulated. Back-table perfusion started immediately thereafter as a cold high-volume/low-pressure perfusion (Perfadex; Vitrolife, Goeteborg, Sweden) at 4°C. Lung lobes were then triple-bagged in cold Perfadex solution and stored on ice. Type II cell preparation started after a cold ischemia time of up to 30 min. The remaining protocol was identical with cell preparation from rat, following lung removal, as described in Ref. 9. Before patch-clamp experiments, human cells subconfluently grown on glass coverslips were identified as type II cells by their typical appearance (multiple large vesicles), and cell viability was confirmed by active, pH-dependent uptake of LysoTracker Green DND-26 into lamellar bodies, as described in Ref. 9. In addition, cell membrane integrity was confirmed by the lack of permeation of the amphiphilic dye FM 1-43 from the bath solution into the cytosol (9).

This protocol has been designed and performed in accordance with the ethical standards in the Declaration of Helsinki and has been reviewed by the ethics committee of the University of Innsbruck.

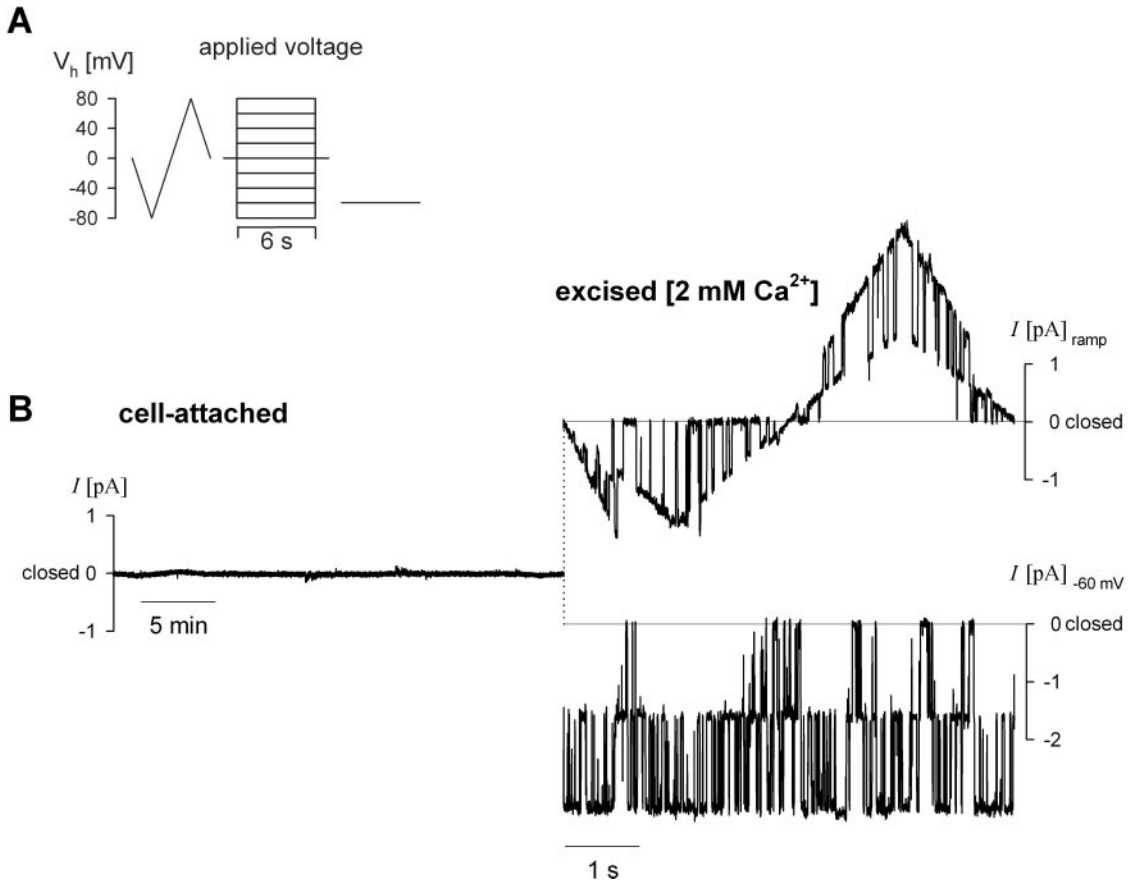

Fig. 1. *A*: holding potential (V_h) protocols used to study $NSC_{Ca/AMP}$ (Ca^{2+}-dependent, nucleotide-inhibited, nonselective, and Ca^{2+}-impermeable cation channel). *B*: excision activation. *B, left*: current recording of a cell-attached membrane patch in an intact type II cell in response to V_h steps and ramps as shown in *A*. No current is detectable. *B, right*: same membrane as *left* after excision to the inside-out (I-O) configuration. The currents (*I*) in response to a V_h ramp (*top* tracing) and during a constant V_h of −60 mV (*bottom* tracing) reveal activation of 2 channels in the patch. Currents were leak corrected.

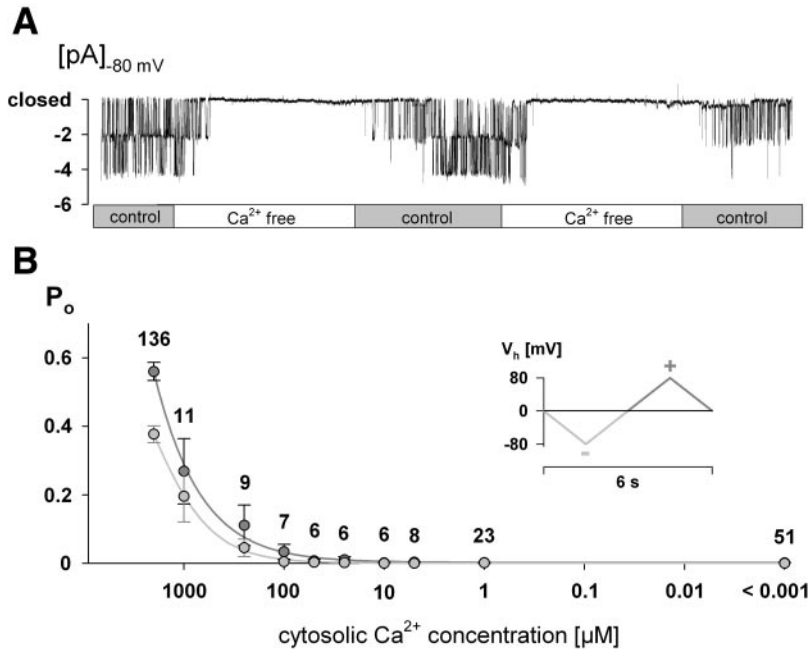

Fig. 2. *A*: on/off switch function of cytoplasmic Ca^{2+}. Current tracing of an excised, I-O membrane patch that was alternatingly exposed to a Ca^{2+}-free and a Ca^{2+}-containing (2 mM) solution. The 2 channels are alternatingly switched off and on. *B*: Ca^{2+} concentration-response relationship. The open probability (P_o) was determined in I-O patches exposed to various cytoplasmic Ca^{2+} concentrations. Dark gray filled circles represent P_o values in the positive V_h range of repetitive ramps (see *inset*); light gray filled circles represent P_o values in the negative V_h range (see *inset*). The maximum Ca^{2+} concentration was 2 mM, because this value is the upper limit that can be expected in vivo for Ca^{2+} concentrations at the cytoplasmic side ($[Ca^{2+}]_{cyt}$) to be reached under maximum cell permeabilization.

Major findings obtained from rat type II cells were subsequently verified in human alveolar type II cells. Common features are listed in Table 1.

Single-channel patch-clamp experiments and fluorescence measurements. Cell-attached and inside-out (I-O) patch-clamp experiments were performed with borosilicate glass patch pipettes of 6- to 7-MΩ resistance and with an EPC9 (HEKA) setup as previously described (21). The I-O configuration was obtained by tearing the patch off the plasma membrane. Unless otherwise stated, the bath solution contained (in mM): 140 NaCl, 5 KCl, 2 $CaCl_2$, 1 $MgCl_2$, 5 D-glucose, and 10 HEPES, pH 7.4 (with NaOH). This control solution was also used as pipette solution unless stated otherwise. Single-channel currents were either recorded at various constant holding potentials (V_h) or during repetitive V_h ramps from −80 to +80 mV and vice versa (Fig. 1). Each ramp lasting for 6 s corresponded to a slope of ±0.053 mV/ms. The open probability (P_o) is defined as the fraction of time during which the channels are in their open state within a patch. P_o was calculated according to

$$P_o = \frac{\Sigma_{n=0}^{N} \frac{t_n}{T}}{N} \quad (1)$$

where t_n is the open time of the channel in the nth level and n is the channel level. T is the total recording time. N is the maximum level of channel opening. P_o was calculated without making any assumption about the total number of channels in a patch or the P_o of a single channel. In experiments where V_h changed periodically (0/−80/0/+80/0), P_o values were separately determined for both the negative (P_o^-) and the positive (P_o^+) cycle of V_h (since single-channel currents are negligibly small near the reversing potential, P_o was not determined for a V_h within the range of ±5.3 mV from the reversal potential).

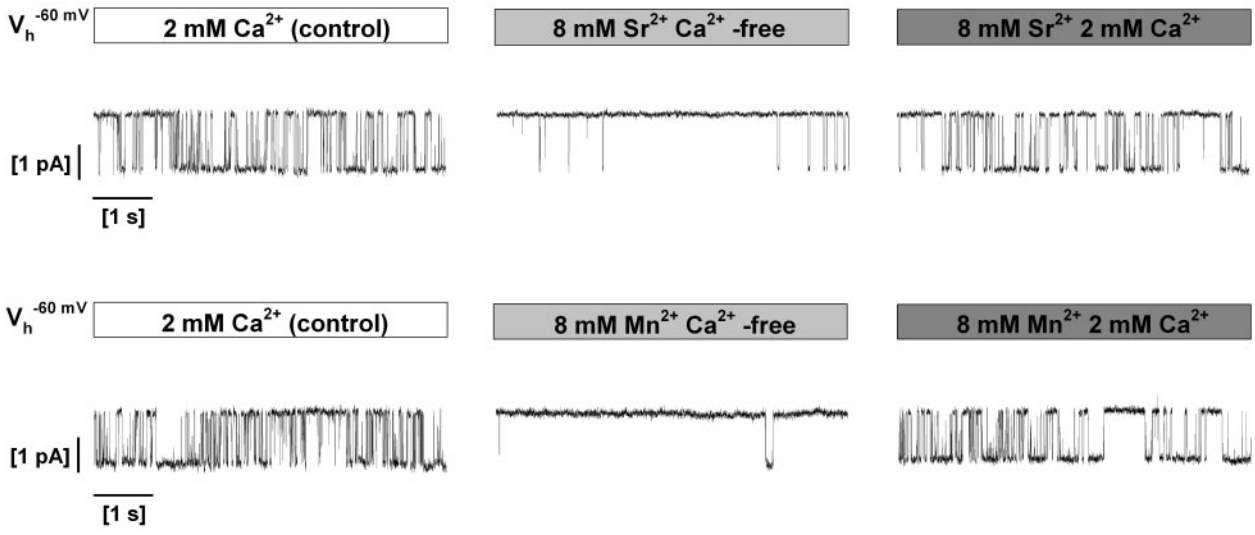

Fig. 3. The effects of cytoplasmic Sr^{2+} and Mn^{2+} in the absence and presence of 2 mM Ca^{2+}. Original current tracings from 2 different I-O patches (*top* vs. *bottom* tracings) are shown (experimental sequence from *left* to *right*). Note that Sr^{2+} or Mn^{2+} can activate the channel to a small extent.

Single-channel currents were sampled at 5 kHz, filtered at 1 kHz with a low-pass Bessel filter, and stored on the hard disk of a PC using the Pulse + PulseFit software (version 8.53, HEKA).

For experiments done in the cell-attached mode, cells were preloaded with fura-2 AM (1.2 μM; Molecular Probes, Leiden, The Netherlands) for 30 min in the incubator. Excitation light of 340-, 380-, and 360-nm wavelengths was applied for 30 ms followed by 6 s of darkness. During illumination, the emitted fura-2 fluorescence was continuously detected by a photomultiplier tube throughout the experiments. The produced current was sampled at a rate of 5 kHz and averaged. The fluorescence signal at the isosbestic point (360 nm) was not Ca^{2+} dependent and was, therefore, taken to assess the integrity of the plasma membrane during the experiment. The ratio signal (340/380 nm) was used to follow changes in $[Ca^{2+}]_{cyt}$. Control of excitation light and data acquisition were performed with the fura extension of the Pulse + PulseFit software (version 8.53, HEKA).

RNA isolation and RT-PCR analysis. Total RNA was isolated from freshly isolated rat type II cells using TriReagent (MRC, Cincinnati, OH). The reverse transcription reaction was performed in a solution of 1 μg RNA, 0.4 mM dNTPs, oligo(dT) primer, and Maloney murine leukemia virus reverse transcriptase (all from Promega, Mannheim, Germany) at 37°C for 60 min. For RT-PCR, 2 μl of template were used.

To design rat transient receptor potential channel, melastatin subfamily (TRPM)4-specific primers, we searched the National Center for Biotechnology Information database (available at www.ncbi.

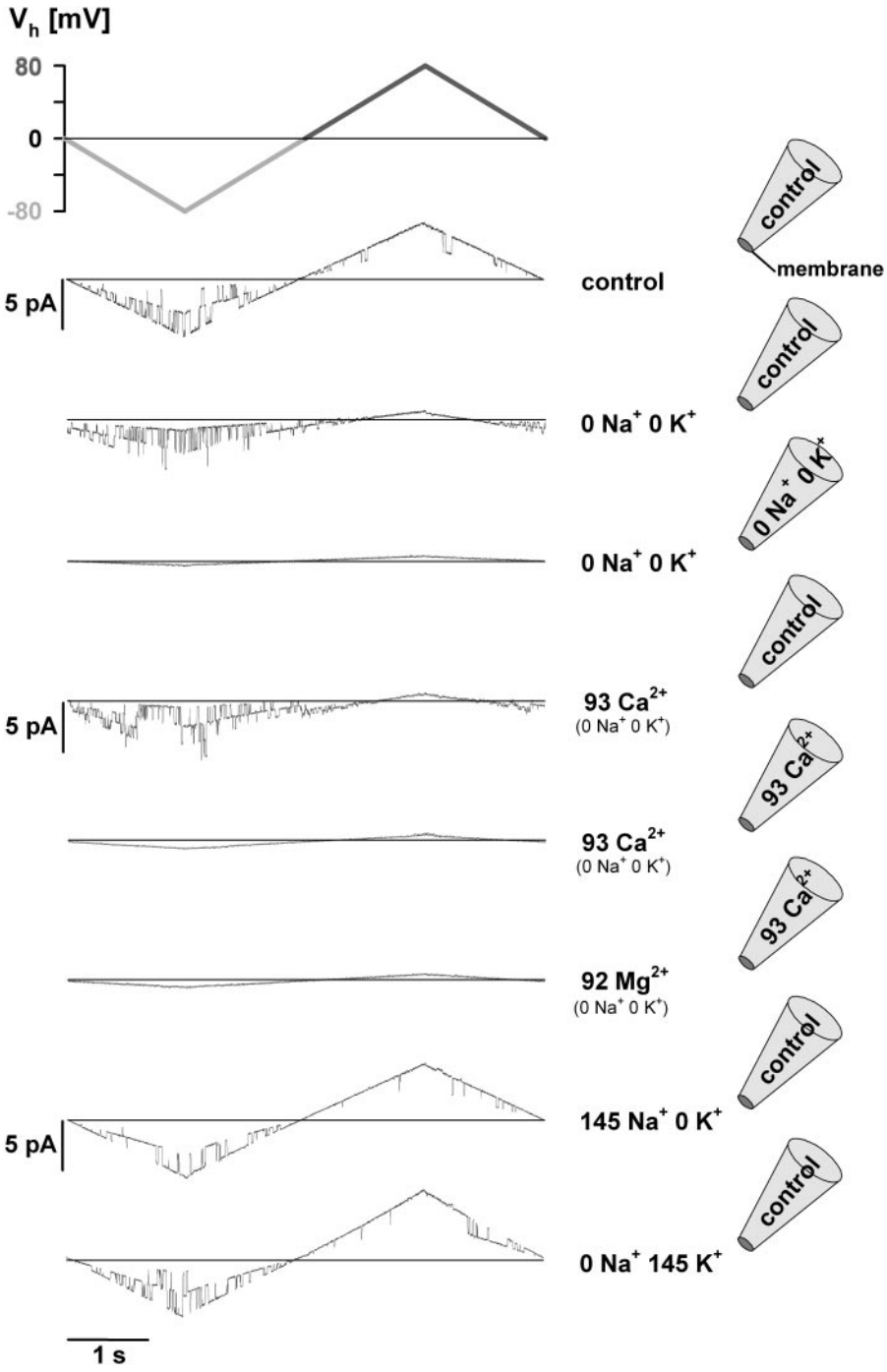

Fig. 4. Examples of ion replacement experiments. Original current recordings (not leak corrected) of I-O patches during V_h ramps as shown above the current recordings. Solutions on both sides of the membrane patch are shown (*right*). A minimum of 2 mM Ca^{2+} at the cytoplasmic side was present in all experiments to maintain channel activity. Note that the current is generated by Na^+ and K^+. The solutions contained (in mM, in addition to 10 HEPES and 5 D-glucose, pH 7.4) for control: 140 NaCl, 5 KCl, 2 $CaCl_2$, and 1 $MgCl_2$; for 0 Na^+ 0 K^+: 145 *N*-methyl-D-glucamine, 2 $CaCl_2$, and 1 $MgCl_2$; for 93 Ca^{2+}: 93 $CaCl_2$ and 1 $MgCl_2$; for 92 Mg^{2+}: 2 $CaCl_2$ and 92 $MgCl_2$; for 145 Na^+ 0 K^+: 145 NaCl, 2 $CaCl_2$, and 1 $MgCl_2$; and for 0 Na^+ 145 K^+: 145 KCl, 2 $CaCl_2$, and 1 $MgCl_2$.

nlm.nih.gov/BLAST) with the mouse TRPM4 sequence (NM_175130) using the tblastN program. The *Rattus norvegicus* chromosome 1 WGS supercontiguous NW_047558 was predicted. Analysis of the NW_047558 sequence leads to the identification of 25 sequence segments that are equivalent to exon 1 to exon 25 of the mouse TRPM4 gene. The rat "exons" cover ~30 kb of the NW_047558 sequence and exhibit ~94% homology to the mouse sequence. Two sets of primer pairs were designed. Primer 1 covers exon 8 to exon 9 forward: 5′-CTCGGCTTACCTGGATGAGC-3′, reverse: 5′-CTCCCAACAGAGTCCTCAG-3′. Primer 2 covers exon 19 to exon 22 forward: 5′-CAGCGACCTCTACTGGAAGG-3′, reverse: 5′-GAGGCAGTAAGGCAGAGTGG-3′. Comparative RT-PCRs were done under the same conditions, and glyceraldehyde phosphodehydrogenase was amplified using published primers (31). The number of PCR cycles was 35.

Materials. Unless stated otherwise, drugs were purchased from SIGMA, Austria.

Statistics. Data are reported as means ± SE. Experiments with no statistical difference between the control and experimental group are mentioned in the text but are not shown as numeric values or as graphs.

RESULTS

Channel expression and Ca^{2+} dependence. No activity of this channel was observed under control conditions, i.e., 6 h up to 5 days after cell isolation, exposed to a control solution in the cell-attached patch-clamp configuration. This lack of channel activity was independent of V_h. Considering a membrane potential of the intact cell of approximately −30 mV (Frick and Mair, unpublished data), clamped potentials correspond to estimated effective potentials between −110 and +50 mV. In contrast, the channel was almost regularly observed after changing from the cell-attached to the I-O patch-clamp configuration under conditions of high $[Ca^{2+}]_{cyt}$ (2 mM, excision activation occurred in ~70% of all I-O patches, as exemplified in Fig. 1). This indicates that the channel is abundantly expressed in type II cells. As shown in Fig. 2, channel activation occurred when $[Ca^{2+}]_{cyt}$ exceeded the nanomolar range. The concentration-response curve suggests that full channel activation was not even obtained when $[Ca^{2+}]_{cyt}$ equaled the extracellular concentration of 2 mM.

Surrogate divalent ions as potential channel activators. The candidates were Sr^{2+}, Mn^{2+}, Mg^{2+}, Ba^{2+}, Co^{2+}, and Cd^{2+}. In these experiments, 8 mM of each surrogate ion were applied to the cytoplasmic side of I-O patches, and Ca^{2+} was omitted (osmolarity was kept constant by adjusting NaCl). Figure 3 demonstrates that Sr^{2+} ($n = 15$) and Mn^{2+} ($n = 16$) could replace Ca^{2+} as channel activator to a certain extent, however, with a dramatically reduced P_o. In contrast, Mg^{2+}, Ba^{2+}, Co^{2+}, and Cd^{2+} were not able to replace Ca^{2+} ($n = 15$, 30, 21, and 11, respectively, data not shown). Readdition of 2 mM Ca^{2+} and omission of the surrogate ions reactivated the channel except for Cd^{2+}, which appeared to block irreversibly (see below). Co^{2+} transiently increased channel activity before channel closure occurred (not shown).

Ion selectivity. Ion replacement experiments (*N*-methyl-D-glucamine$^+$ for Na^+ or K^+, gluconate$^-$ for Cl^-) revealed a high selectivity for K^+ and Na^+ over Cl^- with approximately equal permeabilities for Na^+ and K^+ (Fig. 4). When *N*-methyl-D-glucamine Cl was replaced by equiosmolar amounts of $CaCl_2$ ($n = 18$) or $MgCl_2$ ($n = 10$) in the presence of 2 mM $CaCl_2$, no changes of the current amplitude were observed. Hence, the channel has to be considered Ca^{2+} impermeable.

Current-voltage behavior. P_o in the negative range of a voltage sweep (P_o^-) was significantly lower than in the positive range (P_o^+) (compare Figs. 1 and 4). The mean duration of a single channel opening was significantly longer at positive V_h. In contrast, the channel conductance was slightly smaller in the positive vs. negative V_h range (25.80 ± 0.05 pS and 28.86 ± 0.07 pS, respectively) (Figs. 1 and 4). The product $P_o \times I$ (I represents current) was higher in the positive range (data not shown), suggesting that whole cell currents, if present, would exhibit an outward rectification.

Effects of potential inhibitors. These experiments were performed in the presence of 2 mM $[Ca^{2+}]_{cyt}$. When amiloride (0.5–5 μM) was applied to the bath solution (I-O patch), P_o was not significantly changed ($n = 5$). Likewise, channel activity was not significantly affected by the presence of 1–5 mM amiloride in the patch pipette ($n = 14$, data not shown).

Sr^{2+}, Mn^{2+}, Mg^{2+}, and Ba^{2+} did not block the channel at concentrations of 8 mM in the presence of 2 mM $[Ca^{2+}]_{cyt}$ ($n = 6$, 7, 6, and 7, respectively, data not shown). Co^{2+} even increased the ability of Ca^{2+} to activate the channel and arrested the channel in the open state ($n = 8$, data not shown). Only Cd^{2+} was a very potent channel blocker with an $EC_{50} \approx 55.5$ nM (Fig. 5).

Effects of agonists and intracellular messengers in cell-attached patch-clamp experiments. We tested whether ATP (20 μM), a known Ca^{2+}-dependent purinergic agonist in type II cells, or (−)isoproterenol (10 μM), a cAMP-dependent stimulator of Na^+ transport, could activate the channel on cell, i.e., within the plasma membrane of living type II cells. Agonists were applied in the bath solution. Neither ATP nor (−)isoproterenol activated the channel in cell-attached patches ($n = 18$ and 32, respectively, data not shown), where the presence of this channel was verified at the end of the experiments by excision-activation. Hence, we can clearly state that even though the channel was present within the membrane patch of the pipette, it could not be activated on cell by these

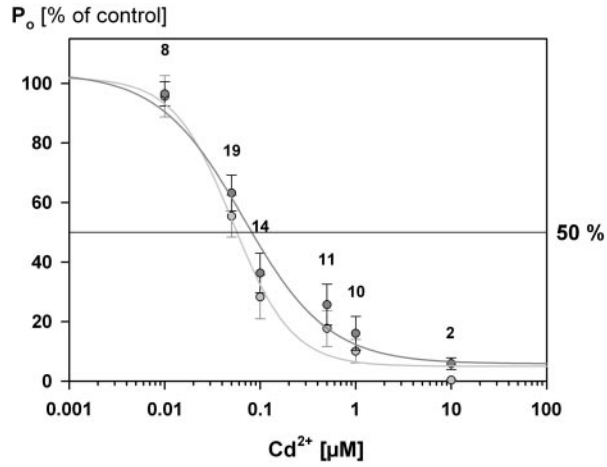

Fig. 5. Cd^{2+} concentration-response relationship. P_o is expressed as % of control (i.e., in the presence of 2 mM bath Ca^{2+} in I-O experiments). As in Fig. 2, light gray filled circles represent values obtained during the negative V_h range of V_h ramps (see Fig. 2*B inset*); $EC_{50} = 67$ nM. Dark gray circles are values from the positive V_h range (see Fig. 2*B inset*); $EC_{50} = 51$ nM; average $EC_{50} = 55.5$ nM. Data were fitted with the general dose-response curve.

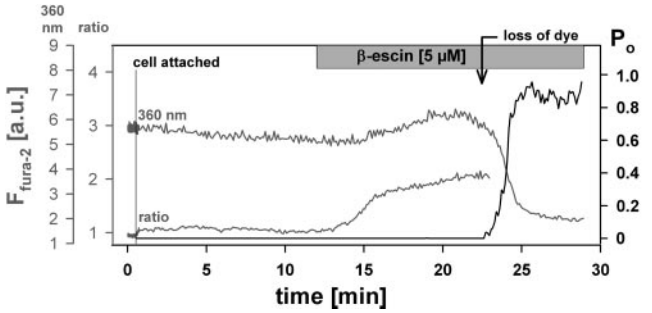

Fig. 6. Permeabilization of the cell membrane during a combined cell-attached patch clamp and fluorescence measurement. F_{fura-2} indicates the fura-2 fluorescence intensity of a single cell under study in arbitrary units (a.u.). The ratio signal indicates the increase of $[Ca^{2+}]_{cyt}$ during treatment with β-escin (indicated above the tracing). The fluorescence tracing at the excitation wavelength of 360 nm (close to the isosbestic point of fura-2) indicates leakage of fura-2 from the cell. The P_o of the channel in the membrane patch is shown in black. Note that $P_o = 0$ up to ~23 min and that it starts to increase when dye leakage becomes significant (beginning of the decline in 360-nm fluorescence).

agonists. The cell-permeable cAMP analog 250 μM dibutyryl adenosine 3′,5′-cyclic monophosphate and the Ca^{2+} ionophore ionomycin (1–10 μM) were also ineffective ($n = 25$ and 15, respectively, not shown), although we know from previous experiments (8) that these concentrations of ionomycin should yield a $[Ca^{2+}]_{cyt}$ far above the threshold of channel activation, as shown in Fig. 2*B*. We therefore speculated that some cytosolic components keep the channel closed even at a high $[Ca^{2+}]_{cyt}$.

To test this hypothesis, we aimed at permeabilizing the plasma membrane to allow leakage and depletion of cytoplasmic compounds. We used β-escin, a saponin derivative extracted from horse chestnuts, which was reported to form holes permeable to high-molecular-weight substances (17). β-Escin (5–40 μM) was added to the bath. In these experiments, the cells were preloaded with fura-2 (see METHODS), and the single cell fura-2 ratio was simultaneously recorded with the channel activity. An example of such an experiment is shown in Fig. 6. In all experiments ($n = 27$), $[Ca^{2+}]_{cyt}$ rose immediately after addition of β-escin, which can be explained as the initiation of permeabilization. Fura-2 leakage from the cell occurred one to several minutes later (Fig. 6) and was dependent on the β-escin concentration. Notably, the beginning of fura-2 leakage coincided with channel activation (Fig. 6). Konishi and Watanabe (17) reported that with a low concentration of β-escin (up to 5 μM), most of the cellular ATP is lost within 30–40 min. Their results demonstrated that β-escin concentrations of 5 μM render the cell membrane permeable to relatively small molecules (ATP) without a substantial loss of large cytosolic proteins. The molecular size of ATP is ~0.5 kDa and that of fura-2 is ~0.65 kDa. We assumed, therefore, that it was the loss of nucleotides that activated the channel (in addition to the high $[Ca^{2+}]_{cyt}$) and tested the hypothesis below.

Effects of nucleotides at the cytoplasmic side of the channel. ATP, ADP, AMP, and adenosine were added to the control bath solution in I-O patch-clamp experiments. The calcium and magnesium ions bound by nucleotides were corrected according to Chang et al. (2) to keep the free $[Ca^{2+}]_{cyt}$ and $[Mg^{2+}]_{cyt}$ constant in all experiments. The results are shown in Fig. 7. The nucleotides blocked the channel in the following order of potency: AMP ≈ ADP > ATP > adenosine (see Fig. 7 legend for EC_{50} values). A comparison of the inhibitory potencies of these and other nucleotides is shown in Fig. 8. cAMP also acted as inhibitor, although not as effectively as ATP or adenosine. GTP had no effect ($n = 14$, Fig. 8).

Hydrolysis is not required for channel inhibition because the nonhydrolyzable ATP analog ATP-γ-S (0.05 mM) reduced P_o even more than the same amount of ATP ($P_o = 40.2 \pm 8.3$ and 61.1 ± 4.9% of control, respectively, $n = 16$ and 19). Adenosine 5′-(β,γ-imido)triphosphate tetralithium salt hydrate (0.5

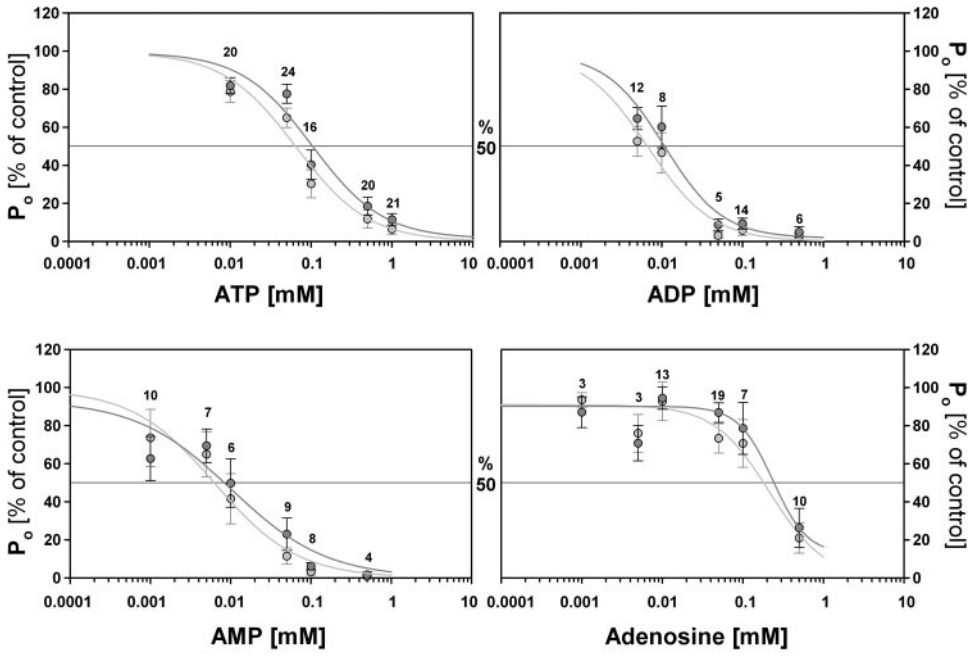

Fig. 7. Nucleotide concentration-response relationship. Nucleotides were added to the bath solution containing 2 mM Ca^{2+} in I-O patch-clamp experiments. (For further details, see Fig. 5.) The EC_{50} values for these substances in the negative and positive V_h range, respectively, are ATP: 64.8 and 103 μM, ADP: 6.7 and 10.7 μM, AMP: 6.3 and 10.1 μM, and adenosine: 211.5 and 235.2 μM. The ranking order in terms of inhibition is AMP = ADP > ATP > adenosine.

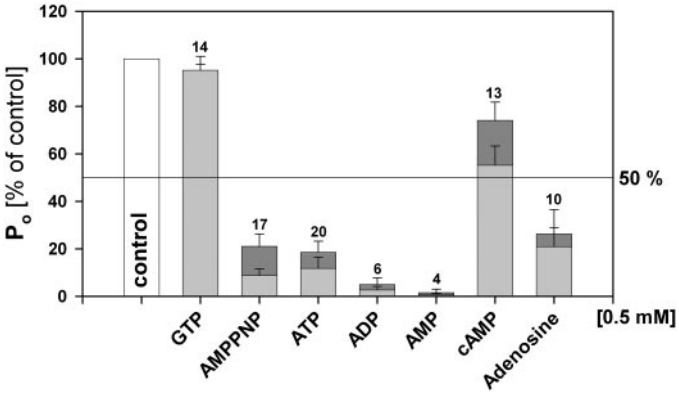

Fig. 8. Comparison of the effects of cytoplasmic adenosine nucleotides, guanosine nucleotides, and adenosine, each given at a concentration of 0.5 mM, on the P_o in I-O patches. Dark and light gray values are as described in Fig. 5. AMPPNP, adenosine 5′-(b,g-imido)triphosphate tetralithium salt hydrate.

mM), another nonhydrolyzable ATP analog, was equally effective ($P_o^- = 8.76 \pm 2.8\%$; $P_o^+ = 21.02 \pm 5.28\%$ of control, $n = 17$, Fig. 8), indicating that ATP hydrolysis is not required for channel inhibition.

A potential role of the cytoskeleton for channel activation was also examined. Preincubation with 1 μM latrunculin B, which inhibits actin polymerization and disrupts microfilament organization, did not result in channel activation in cell-attached patches ($n = 15$). Nocodazol, a tubulin depolymerization promoter, also had no effect.

Expression of rat TRPM4b. The efficiency of nucleotide inhibition and other features of $NSC_{Ca/AMP}$ resemble a recently described splice variant of the TRPM4 channel TRPM4b, where TRPM stands for transient receptor potential channel, melastatin subfamily. We analyzed TRPM4b by RT-PCR in two independent preparations of rat type II cells. Two primer pairs were used: primer 1 amplified a 365-bp product from exon 8 to exon 9 of the rat TRPM4 gene, and primer 2 amplified a 443-bp product from exon 19 to exon 22, respectively. Importantly, the amplified products cannot stem from genomic DNA since the primers cross exon/intron boundaries. As shown in Fig. 9, both PCR products could be amplified from type II cells, demonstrating that the TRPM4b gene is expressed.

DISCUSSION

The major differences between $NSC_{Ca/AMP}$ and other published cation channels in type II cells are its inactivity under normal physiological conditions, its amiloride insensitivity, and the lack of (−)isoproterenol or cAMP-dependent activation, but, instead, nucleotide-dependent inhibition. With regard to both features, $NSC_{Ca/AMP}$ is certainly different from a 20- to 25-pS channel purified from type II cells and reconstituted in lipid bilayers, because in this channel, ATP at the cytoplasmic side did not have an inhibitory effect (36). Furthermore, since $NSC_{Ca/AMP}$ is clearly not activated by the cAMP pathway, it is different from cation channels involved in cAMP-dependent, transepithelial Na^+ reabsorption.

Despite its Ca^{2+} dependence, $NSC_{Ca/AMP}$ was never activated on cell by extracellular ATP, although this agonist evokes an elevation of $[Ca^{2+}]_{cyt}$ in type II cells that is usually >500 nM (8) and hence in the range where channel openings should be observed. All evidence presented here suggests that this is due to a strong inhibition by cytoplasmic adenine nucleotides, overriding potential activation by Ca^{2+}. This is another argument that the channel is different from nonselective cation channels associated with transport because these channels are spontaneously active on cell (42). Importantly, the abundance and features of $NSC_{Ca/AMP}$ did not change within a time frame between a few hours and many days after cell preparation, which is also different from channels involved in transport (13). Taking together all these differences, it appears justified to conclude that $NSC_{Ca/AMP}$ has an entirely different function than transepithelial transport and is "silent" under conditions when transport channels may be fully or partially active.

$NSC_{Ca/AMP}$ channels of identical or similar characteristics have been described in various cell types, such as brown adipocytes (10, 16), pancreatic β-cells (34, 38), kidney epithelium (18, 30), and eye (corneal) endothelium (33). Until now, neither clear structural nor functional information has been available about them. Recently, however, a subtype of the TRP channel family TRPM4b (in contrast to the short splice variant TRPM4a) with striking similarities to $NSC_{Ca/AMP}$ was expressed in HEK cells (19, 26). This channel is also cation selective, Ca^{2+} impermeable, Ca^{2+} dependent, and inhibited

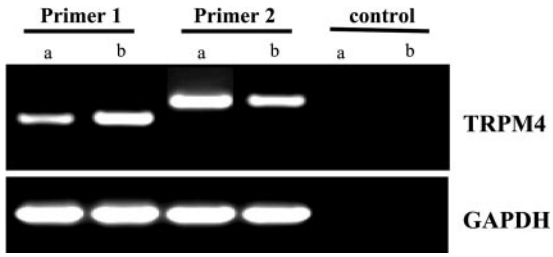

Fig. 9. Expression of transient receptor potential channel, melastatin subfamily (TRPM)4. RT-PCR of 2 independent preparations of type II cells (a and b). Two PCR products specific for rat TRPM4 were detected: primer 1 amplified a 365-bp fragment, and primer 2 amplified a 443-bp fragment. For controls, RT-PCR was performed without reverse transcriptase.

Table 2. *Comparison of properties of $NSC_{Ca/AMP}$*

	$NSC_{Ca/AMP}$	TRPM4b
Single-channel conductance, *I-V* relationship	26–29 pS, almost linear	25 pS, almost linear
Open probability	Outwardly rectifying	Outwardly rectifying
Permability	K^+ and Na^+, not Ca^{2+}	K^+ and Na^+, not Ca^{2+}
Activation by Ca^{2+}	>100 nM	>100 nM
Ca^{2+} substitution for channel activation	Sr^{2+}, not Ba^{2+}	Sr^{2+}, not Ba^{2+}
Inhibition by ATP	$EC_{50} \approx 100$ μM	$EC_{50} \approx 10$ μM
Inhibition by ADP	$EC_{50} \approx 10$ μM	$EC_{50} \approx 2$ μM
Inhibition by AMP	$EC_{50} \approx 10$ μM	$EC_{50} \approx$ 20–200 μM
Inhibition by adenosine	$EC_{50} \approx 200$ μM	$EC_{50} \approx 600$ μM
Inhibition by Cd^{2+}	$EC_{50} \approx 55$ nM	n.d.
cAMP	Mild inhibition	Ineffective

Comparison of the properties of $NSC_{Ca/AMP}$ reported here with TRPM4b, as published in Refs. 19 and 26. n.d., Not determined; $NSC_{Ca/AMP}$, Ca^{2+}-dependent, nucleotide-inhibited, nonselective, and Ca^{2+}-impermeable cation channel; TRPM, transient receptor potential channel, melastatin subfamily; *I-V,* current-voltage.

by nucleotides in the micromolar range (19, 26). A detailed comparison between $NSC_{Ca/AMP}$ and TRPM4b is presented in Table 2. Hence, TRPM4b is a very strong candidate for $NSC_{Ca/AMP}$. Consistently, our RT-PCR experiments indicate that this channel is indeed expressed in type II cells. The appearance of multiple channels within one excised membrane patch is also consistent with the reported ability of TRPM4b to homoassociate and form homomultimeric channels (19).

Potential roles of $NSC_{Ca/AMP}$. Expression of $NSC_{Ca/AMP}$ in various cell types suggests involvement in a function that is common to cells of different origin and specialization. As long as the physiological (pathophysiological?) mode of activation of this channel remains obscure, we can only speculate about its role. Importantly, the cell permeabilization experiments with β-escin definitely rule out that excision activation (I-O patch) was a result of a physical disruption between the channel and cellular components (such as channel-anchoring elements).

In HEK-293 cells overexpressing TRPM4b, Launay et al. (19) reported transient TRPM4b channel activation on cell in an experimental setting where Ca^{2+} entry was greatly supported by a high, negative holding potential and simultaneous activation of store-operated Ca^{2+} influx. Unfortunately, these results are difficult to interpret, because their patch pipette-filling solution did not contain ATP, and actual cytoplasmic nucleotide concentrations are impossible to estimate. They suggested that localized (subplasmalemmal) rather than global Ca^{2+} concentrations would be able to activate TRPM4b, inducing oscillatory depolarizations of the membrane potential, thereby reducing the electrical driving force for Ca^{2+} entry and "fine-tuning" capacitative Ca^{2+} entry. This model implies a very close vicinity between a Ca^{2+}-permeable channel and TRPM4b, where TRPM4b exerts a voltage-mediated negative feedback control on Ca^{2+} entry. If this hypothesis holds true for type II cells, TRPM4b might play an important protective role in the alveolus by preventing cellular Ca^{2+} overload during various types of stimulation. Because Ca^{2+}-permeable cation channels are also considered to be involved in apoptosis (39), $NSC_{Ca/AMP}$ could be, in analogy to its potential role as "anticapacitative Ca^{2+} entry channel," an "antiapoptosis channel." It should be noted that the inability to activate $NSC_{Ca/AMP}$ on cell by agonists in our study may be due to a relatively low membrane potential of isolated type II cells (~−30 mV, see above). This constitutes an unfavorable condition (small driving force) for agonist-induced (capacitative) Ca^{2+} entry, and hence, subplasmalemmal Ca^{2+} concentrations needed to activate $NSC_{Ca/AMP}$ in cell-attached patches may be even more difficult to generate.

On the basis of the same considerations, Nilius et al. (26) suggested that TRPM4b might play a protective role during metabolic injury by slowing down Ca^{2+} entry and Ca^{2+}-dependent metabolic processes. This prima vista appealing hypothesis suffers from the lack of a conceivable metabolic situation in which all three nucleotides (ATP, ADP, and AMP) should be depleted.

The main function of type II cells is the production and secretion of surfactant via exocytosis of lamellar bodies. Because exocytosis is an ubiqitous process, the widespread expression of $NSC_{Ca/AMP}$ would be consistent with a role therein. It is unclear, however, how a Ca^{2+}-impermeable cation channel could contribute to membrane fusion or fusion pore expansion. Consistent with its presumed Ca^{2+} entry-inhibiting function (see above), it would impede rather than stimulate surfactant secretion in type II cells, in particular when caused by cell strain, which is critically dependent on Ca^{2+} entry (6).

Korbmacher et al. (18) speculated that a similar cation channel in kidney collecting duct cells may be involved in volume regulation. We tested a potential mechanosensitivity by applying suction to the patch pipette. Channel activation was not detected under this condition (data not shown).

It appears that nucleotides are used by nature as constant, "reliable" inhibitors of this channel, preventing a fatal breakdown of the membrane potential under "normal" conditions. The search for a physiological situation where such inhibition is overridden in the type II cell (see above) will be necessary to gain more insight into its role in the lung. Beyond Ca^{2+} microdomains, hypothetical nucleotide-free cytoplasmic zones and potential cellular components in addition to Ca^{2+}, which could overcome nucleotide inhibition, should be considered.

ACKNOWLEDGMENTS

We thank Gabriele Buemberger for proofreading the manuscript. Technical assistance by Gerlinde Siber and Irina Öttl is gratefully acknowledged.

GRANTS

This work was supported by the Fonds zur Förderung der Wissenschaftlichen Forschung (FWF) Grants P15742 and P15743, Austrian National Bank Grant 9640, Fonds zur Förderung der Forschung an den Universitätskliniken Innsbruck Grant 16, and the Austrian Ministry of Science GZ 140.139/1-VI/Ia/2002.

REFERENCES

1. **Berdiev BK, Shlyonsky VG, Senyk O, Keeton D, Guo Y, Matalon S, Cantiello HF, Prat AG, Ausiello DA, Ismailov II, and Benos DJ.** Protein kinase A phosphorylation and G protein regulation of type II pneumocyte Na^+ channels in lipid bilayers. *Am J Physiol Cell Physiol* 272: C1262–C1270, 1997.
2. **Chang D, Hsieh PS, and Dawson DC.** Calcium: a program in BASIC for calculating the composition of solutions with specified free concentrations of calcium, magnesium and other divalent cations. *Comput Biol Med* 18: 351–366, 1988.
3. **Chen XJ, Eaton DC, and Jain L.** β-Adrenergic regulation of amiloride-sensitive lung sodium channels. *Am J Physiol Lung Cell Mol Physiol* 282: L609–L620, 2002.
4. **Dobbs LG, Gonzalez R, and Williams MC.** An improved method for isolating type II cells in high yield and purity. *Am Rev Respir Dis* 134: 141–145, 1986.
5. **Feng ZP, Clark RB, and Berthiaume Y.** Identification of nonselective cation channels in cultured adult rat alveolar type II cells. *Am J Respir Cell Mol Biol* 9: 248–254, 1993.
6. **Frick M, Bertocchi C, Jennings P, Haller T, Mair N, Singer W, Pfaller W, Ritsch-Marte M, and Dietl P.** Ca^{2+} entry is essential for cell strain-induced lamellar body fusion in isolated rat type II pneumocytes. *Am J Physiol Lung Cell Mol Physiol* 286: L210–L220, 2004.
7. **Garty H and Palmer LG.** Epithelial sodium channels: function, structure, and regulation. *Physiol Rev* 77: 359–396, 1997.
8. **Haller T, Auktor K, Frick M, Mair N, and Dietl P.** Threshold calcium levels for lamellar body exocytosis in type II pneumocytes. *Am J Physiol Lung Cell Mol Physiol* 277: L893–L900, 1999.
9. **Haller T, Ortmayr J, Friedrich F, Volkl H, and Dietl P.** Dynamics of surfactant release in alveolar type II cells. *Proc Natl Acad Sci USA* 95: 1579–1584, 1998.
10. **Halonen J and Nedergaard J.** Adenosine 5′-monophosphate is a selective inhibitor of the brown adipocyte nonselective cation channel. *J Membr Biol* 188: 183–197, 2002.
11. **Hummler E, Barker P, Gatzy J, Beermann F, Verdumo C, Schmidt A, Boucher R, and Rossier BC.** Early death due to defective neonatal lung liquid clearance in α-ENaC-deficient mice. *Nat Genet* 12: 325–328, 1996.

12. **Jain L, Chen XJ, Malik B, Al Khalili O, and Eaton DC.** Antisense oligonucleotides against the α-subunit of ENaC decrease lung epithelial cation-channel activity. *Am J Physiol Lung Cell Mol Physiol* 276: L1046–L1051, 1999.
13. **Jain L, Chen XJ, Ramosevac S, Brown LA, and Eaton DC.** Expression of highly selective sodium channels in alveolar type II cells is determined by culture conditions. *Am J Physiol Lung Cell Mol Physiol* 280: L646–L658, 2001.
14. **Johnson MD, Widdicombe JH, Allen L, Barbry P, and Dobbs LG.** Alveolar epithelial type I cells contain transport proteins and transport sodium, supporting an active role for type I cells in regulation of lung liquid homeostasis. *Proc Natl Acad Sci USA* 99: 1966–1971, 2002.
15. **Kemp PJ, Borok Z, Kim KJ, Lubman RL, Danto SI, and Crandall ED.** Epidermal growth factor regulation in adult rat alveolar type II cells of amiloride-sensitive cation channels. *Am J Physiol Cell Physiol* 277: C1058–C1065, 1999.
16. **Koivisto A, Klinge A, Nedergaard J, and Siemen D.** Regulation of the activity of 27 pS nonselective cation channels in excised membrane patches from rat brown-fat cells. *Cell Physiol Biochem* 8: 231–245, 1998.
17. **Konishi M and Watanabe M.** Molecular size-dependent leakage of intracellular molecules from frog skeletal muscle fibers permeabilized with β-escin. *Pflügers Arch* 429: 598–600, 1995.
18. **Korbmacher C, Volk T, Segal AS, Boulpaep EL, and Fromter E.** A calcium-activated and nucleotide-sensitive nonselective cation channel in M-1 mouse cortical collecting duct cells. *J Membr Biol* 146: 29–45, 1995.
19. **Launay P, Fleig A, Perraud AL, Scharenberg AM, Penner R, and Kinet JP.** TRPM4 is a Ca^{2+}-activated nonselective cation channel mediating cell membrane depolarization. *Cell* 109: 397–407, 2002.
20. **Lazrak A, Nielsen VG, and Matalon S.** Mechanisms of increased Na^+ transport in ATII cells by cAMP: we agree to disagree and do more experiments. *Am J Physiol Lung Cell Mol Physiol* 278: L233–L238, 2000.
21. **Mair N, Haller T, and Dietl P.** Exocytosis in alveolar type II cells revealed by cell capacitance and fluorescence measurements. *Am J Physiol Lung Cell Mol Physiol* 276: L376–L382, 1999.
22. **Margreiter R, Konigsrainer A, Schmid T, Takahashi N, Pernthaler H, and Ofner D.** Multiple organ procurement–a simple and safe procedure. *Transplant Proc* 23: 2307–2308, 1991.
23. **Matalon S, Lazrak A, Jain L, and Eaton DC.** Invited Review: Biophysical properties of sodium channels in lung alveolar epithelial cells. *J Appl Physiol* 93: 1852–1859, 2002.
24. **Matalon S and O'Brodovich H.** Sodium channels in alveolar epithelial cells: molecular characterization, biophysical properties, and physiological significance. *Annu Rev Physiol* 61: 627–661, 1999.
25. **Matthay MA, Folkesson HG, and Clerici C.** Lung epithelial fluid transport and the resolution of pulmonary edema. *Physiol Rev* 82: 569–600, 2002.
26. **Nilius B, Prenen J, Voets T, and Droogmans G.** Intracellular nucleotides and polyamines inhibit the Ca^{2+}-activated cation channel TRPM4b. *Pflügers Arch* 448: 70–75, 2004.
27. **Norlin A, Lu LN, Guggino SE, Matthay MA, and Folkesson HG.** Contribution of amiloride-insensitive pathways to alveolar fluid clearance in adult rats. *J Appl Physiol* 90: 1489–1496, 2001.
28. **O'Grady SM and Lee SY.** Chloride and potassium channel function in alveolar epithelial cells. *Am J Physiol Lung Cell Mol Physiol* 284: L689–L700, 2003.
29. **Orser BA, Bertlik M, Fedorko L, and O'Brodovich H.** Cation selective channel in fetal alveolar type II epithelium. *Biochim Biophys Acta* 1094: 19–26, 1991.
30. **Paulais M and Teulon J.** A cation channel in the thick ascending limb of Henle's loop of the mouse kidney: inhibition by adenine nucleotides. *J Physiol* 413: 315–327, 1989.
31. **Pirkebner D, Fuetsch M, Wittmann W, Weiss H, Haller T, Schramek H, Margreiter R, and Amberger A.** Reduction of intracellular pH inhibits constitutive expression of cyclooxygenase-2 in human colon cancer cells. *J Cell Physiol* 198: 295–301, 2004.
32. **Pitkanen OM and O'Brodovich HM.** Significance of ion transport during lung development and in respiratory disease of the newborn. *Ann Med* 30: 134–142, 1998.
33. **Rae JL, Dewey J, Cooper K, and Gates P.** A non-selective cation channel in rabbit corneal endothelium activated by internal calcium and inhibited by internal ATP. *Exp Eye Res* 50: 373–384, 1990.
34. **Reale V, Hales CN, and Ashford ML.** Nucleotide regulation of a calcium-activated cation channel in the rat insulinoma cell line, CRI-G1. *J Membr Biol* 141: 101–112, 1994.
35. **Rossier BC, Canessa CM, Schild L, and Horisberger JD.** Epithelial sodium channels. *Curr Opin Nephrol Hypertens* 3: 487–496, 1994.
36. **Senyk O, Ismailov I, Bradford AL, Baker RR, Matalon S, and Benos DJ.** Reconstitution of immunopurified alveolar type II cell Na^+ channel protein into planar lipid bilayers. *Am J Physiol Cell Physiol* 268: C1148–C1156, 1995.
37. **Snyder PM, Cheng C, Prince LS, Rogers JC, and Welsh MJ.** Electrophysiological and biochemical evidence that DEG/ENaC cation channels are composed of nine subunits. *J Biol Chem* 273: 681–684, 1998.
38. **Sturgess NC, Hales CN, and Ashford ML.** Inhibition of a calcium-activated, non-selective cation channel, in a rat insulinoma cell line, by adenine derivatives. *FEBS Lett* 208: 397–400, 1986.
39. **Szabo I, Adams C, and Gulbins E.** Ion channels and membrane rafts in apoptosis. *Pflügers Arch* 448: 304–312, 2004.
40. **Widdcombe JH.** How does cAMP increase active Na absorption across alveolar epithelium? *Am J Physiol Lung Cell Mol Physiol* 278: L231–L232, 2000.
41. **Yue G, Hu P, Oh Y, Jilling T, Shoemaker RL, Benos DJ, Cragoe EJ Jr, and Matalon S.** Culture-induced alterations in alveolar type II cell Na^+ conductance. *Am J Physiol Cell Physiol* 265: C630–C640, 1993.
42. **Yue G, Shoemaker RL, and Matalon S.** Regulation of low-amiloride-affinity sodium channels in alveolar type II cells. *Am J Physiol Lung Cell Mol Physiol* 267: L94–L100, 1994.